

Vibrations in submonolayer structures of Na on Cu(111)S. D. Borisova,¹ G. G. Rusina,¹ S. V. Eremeev,¹ G. Benedek,² P. M. Echenique,^{3,4} I. Yu. Sklyadneva,^{1,3} and E. V. Chulkov^{3,4,*}¹*Institute of Strength Physics and Materials Science, prospekt Akademicheskii 2/1, 634021, Tomsk, Russia*²*Dipartimento di Scienza dei Materiali, Università di Milano-Bicocca, Via Cozzi 53, 20125 Milano, Italy*³*Donostia International Physics Center (DIPC), Paseo de Manuel Lardizabal 4, 20018 San Sebastián/Donostia, Basque Country, Spain*⁴*Departamento de Física de Materiales and Centro Mixto CSIC-UPV/EHU, Facultad de Ciencias Químicas, Universidad del País Vasco Euskal Herriko Unibertsitatea, Apartado 1072, 20080 San Sebastián/Donostia, Basque Country, Spain*

(Received 14 April 2006; revised manuscript received 8 August 2006; published 23 October 2006)

We present the results of a comparative study of the equilibrium crystal structure and vibrational properties of the Na/Cu(111) system at coverages up to monolayer saturation. The calculations are performed with interaction potentials from the embedded-atom method. The following ordered structures are considered: $p(3 \times 3)$, $p(2 \times 2)$, $(\sqrt{3} \times \sqrt{3})30^\circ$, and $(3/2 \times 3/2)$. The surface relaxation, phonon dispersion, and polarization of vibrational modes for the adsorbate and substrate atoms as well as the local density of states are discussed. It is found that the bond length between an adsorbate and the nearest-neighbor substrate atom slightly increases with increasing coverage. Adsorption of sodium also results in a small rumpling in two upper substrate layers. The mode associated with adatom-substrate stretch vibrations was obtained in our calculation at about 22 meV for all the structures considered. The strength of this mode decreases with increasing coverage in accordance with the experiment. On the other hand, we find that the frustrated translation mode frequency of sodium on Cu(111) is strongly coverage dependent.

DOI: [10.1103/PhysRevB.74.165412](https://doi.org/10.1103/PhysRevB.74.165412)

PACS number(s): 68.43.Pq, 63.20.Dj, 63.22.+m, 68.35.Ja

I. INTRODUCTION

Adsorption of alkali-metal atoms on metal surfaces causes a drastic change of many properties of metal substrate surfaces. In particular, this adsorption frequently results in the formation of complex crystal structures which involve a certain restructuring of the substrate surface atoms.¹⁻³ It leads to the modification of the substrate surface electronic states^{4,5} and gives rise to adsorbate- (adlayer-)induced electron states.⁴⁻¹⁰ The formation of submonolayer structures on metals influences electron-electron^{11,12} and electron-phonon^{8,12-14} scattering in excited electron and hole states, leading often to a change of the decay mechanisms of an excited electron or/and hole.¹⁵ It also gives rise to new vibrational states related to the adatoms.¹⁶⁻¹⁸

Extensive studies have been performed for alkali-metal atoms on aluminium surfaces. In addition to experiments and theoretical calculations that focused on electronic properties of the adsorbate-induced phases, the structural characteristics as well as the influence of adsorbate-substrate and adsorbate-adsorbate interactions on the vibrational properties have been intensively investigated.^{5,16-18} As for Na adatoms on the Cu(111) surface, so far the adsorption structures at coverages below the saturated monolayer (ML) remain uncertain though adsorbate-induced systems have been studied by different experimental techniques.^{3,19-23} At saturated monolayer coverages, alkali-metal atoms adsorbed on close-packed (111) metal surfaces generally form hexagonal structures.³ For Na adsorption, the monolayer saturation occurs at a coverage of $\theta \approx 0.44$ (the coverage is defined as the ratio of Na adatoms to the number of Cu surface atoms) when the Na adatoms form a hexagonal $(3/2 \times 3/2)$ structure with Na-Na spacing close to that in the bulk sodium.^{3,21-23} At low coverages, low-energy electron diffraction experiments report either an ordered hexagonal $p(2 \times 2)$ structure at $\theta \approx 0.25$,^{19,20}

or less ordered adsorbate phases up to monolayer saturation.²¹ A low-temperature scanning tunneling microscopy study²³ showed that already at coverages of $\theta \approx 0.11$ (0.25 ML) the Na atoms locally formed a $p(3 \times 3)$ hexagonal phase with one atom per unit cell. To describe the transition from the $p(3 \times 3)$ low-coverage structure to the $(3/2 \times 3/2)$ with four atoms per unit cell in the saturated monolayer, Kliewer and Berndt have suggested a model derived from an analysis of the electronic structure of the Na films. This transition includes some intermediate phases such as a mixing of $p(3 \times 3)$ and $p(2 \times 2)$ structures up to a coverage of $\theta \approx 0.25$ (0.56 ML) and the formation of a $(\sqrt{3} \times \sqrt{3})30^\circ$ structure with three atoms per unit cell at $\theta \approx 0.33$ (0.75 ML). However, the adsorption site preference of Na adatoms on Cu(111) has not been revealed yet experimentally. These data are available for heavier alkali-metal atoms, K, Cs, and Rb, on Cu(111).²⁴⁻²⁶ It was reported that these adsorbates occupy on-top sites. For Li and Na adsorption, the work function change and the coverage dependence of the work function are found to be similar to those observed for the heavier alkali metals.²⁷ These similarities indicate that both Li and Na adatoms occupy on-top or hollow sites rather than substitutional ones. For Li on Cu(111), according to the experiments, substitution intermixing with substrate atoms occurs only beyond monolayer coverage.^{27,28} No experimental evidence of the intermixing between sodium adatoms and copper substrate atoms is available. Cluster calculations for a single sodium atom adsorbed on the Cu(111) surface²⁹ do not show whether the Na adatoms occupy on-top sites or reside in hollow sites. Later, the geometries of the $p(2 \times 2)$ and $(3/2 \times 3/2)$ ordered adsorption structures on the Cu(111) surface were investigated by comparing the binding energies of the Na adlayer at different high-symmetry sites.⁹ It was found that the Na adatoms have a slight preference for adsorption in hollow sites at least in the case of the $p(2 \times 2)$

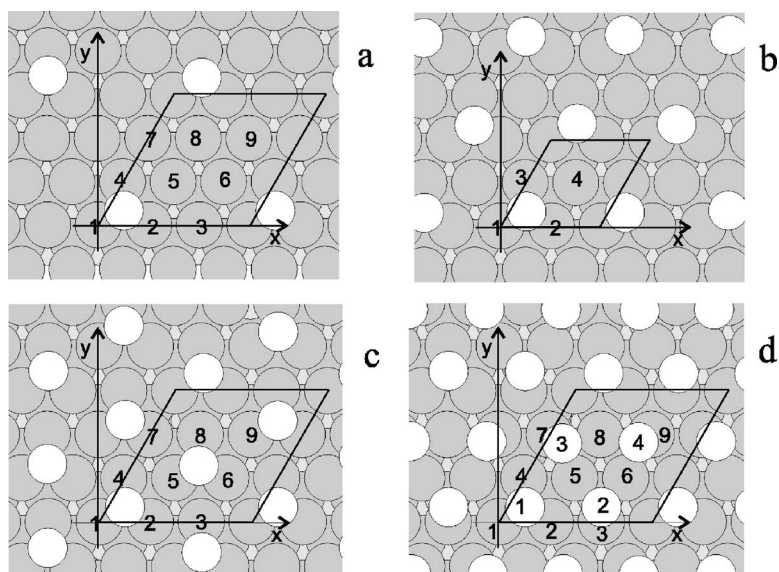


FIG. 1. Adsorption structures (a) $p(3 \times 3)$, (b) $p(2 \times 2)$, (c) $(\sqrt{3} \times \sqrt{3})$, and (d) $(3/2 \times 3/2)$. The supercell is indicated by a rhombus. The numbered copper topmost layer atoms (gray circles) and sodium adatoms (white circles) belong to the unit cell (see the text). Here $x=[1\bar{1}0]$ and $y=[11\bar{2}]$.

structure, in contrast to the heavier alkali metals, which prefer on-top positions.^{3,24–26} However, the differences in the binding energy between hollow and bridge sites are very small, only a few meV. For fcc and hcp adsorption positions the obtained values of the binding energy are the same. In the case of the $(3/2 \times 3/2)$ phase, the calculated binding energies were found to be comparable for top or bridge and for hollow adsorption, which indicates a weak site preference for Na adatoms.

As for the vibrational properties, the phonon dispersion curves have been measured using He scattering^{30,31} for Na films on Cu(001) made of 1–30 ML, and then analyzed within the framework of a force constant model.³² For Na atoms absorbed on the Cu(111) surface, the frequency and intensity of adatom-substrate stretch vibrations have been measured using electron-energy-loss spectroscopy (EELS).^{33–36} The vibrational energy of the stretching (S) mode was found to be ≈ 21 meV and almost independent of the coverage within the range of 0–0.35 ML, whereas the intensity appeared to be strongly coverage dependent, with a maximum at about 0.15 ML. It is known that a nearly constant S mode energy is a common feature of alkali-metal adsorption on close-packed surfaces.^{27,34} At monolayer saturation experimental data are available only for Na/Cu(100), where the S mode vibrational energy is ≈ 18 meV.³⁰ On the other hand, the frustrated translation (T) mode of Na on Cu(001) was shown to be strongly dependent on coverage³⁷ with, however, a negligible dispersion. In *ab initio* calculations of a monolayer Na film on Cu(111),¹³ the adatom-substrate stretch energy of 21 meV was obtained from the curvature of the total energy with respect to the displacement of a rigid adlayer relative to a rigid substrate. Taking into account the influence of the substrate lattice dynamics, the value of 18 meV was obtained. Thus, for Na adatoms on Cu(111), the frequency of an adatom-substrate stretch vibration is the only available value so far. Another motivation of our work is to check whether the approximation of rigid Na adlayer vibrations characterized by one frequency ω_0 only¹³ (Einstein mode) could be valid to represent the entire phonon spectrum of 1 ML of Na on Cu(111).

In this paper, we present the results of a detailed comparative theoretical study of the equilibrium crystal structure and vibrational properties of the Na/Cu(111) system at coverages up to monolayer saturation. We have considered the following ordered structures: $p(3 \times 3)$, $p(2 \times 2)$, $(\sqrt{3} \times \sqrt{3})30^\circ$, and $(3/2 \times 3/2)$. To simplify the comparison of the calculated vibrational properties of the $(\sqrt{3} \times \sqrt{3})30^\circ$ structure with those of the other ordered phases, we use for the former a unit cell (3×3) [see Fig. 1(c)]. The surface relaxation and phonon dispersion curves as well as the local density of states are analyzed. The paper is organized as follows. A short outline of the calculation methods is given in Sec. II. In Sec. III we present and discuss in detail the calculation results. Finally the conclusions are drawn in Sec. IV.

II. COMPUTATIONAL METHOD

The calculations are performed using the embedded-atom method³⁸ (EAM) for the description of the interatomic interaction potentials Cu-Cu and Na-Na. Parameters of the method are determined by fitting to experimental data such as the equilibrium lattice constant, elastic constants, sublimation energy, and vacancy formation energy of the pure bulk metals. These EAM interatomic potentials were applied before to the calculation of phonons on clean surfaces of Na (Ref. 39) and Cu.⁴⁰ The interaction between Cu and Na atoms is described by a pair potential constructed in the form proposed in Ref. 41:

$$\phi_{\text{Cu-Na}}(r) = \frac{1}{2} \left(\frac{\rho_{\text{Na}}}{\rho_{\text{Cu}}} \phi_{\text{Cu}}(r) + \frac{\rho_{\text{Cu}}}{\rho_{\text{Na}}} \phi_{\text{Na}}(r) \right),$$

where $\rho_{\text{Cu(Na)}}$ is the electron density at a Cu (Na) atom site formed by superposition of the electron densities of all other Cu (Na) atoms of the corresponding bulk metal; $\phi_{\text{Cu(Na)}}$ is the pair interaction potential Cu-Cu (Na-Na).

To obtain the equilibrium configuration we relax the surfaces with adsorbates using standard molecular-dynamics technique based on the calculated EAM interaction poten-

tials. The evaluations of vibrational spectra are carried out in the thin film model. We use a two-dimensional periodic slab consisting of 31 atomic layers of Cu. This thickness is sufficient to avoid interactions between two opposite surfaces of the slab. The supercell for the $p(3 \times 3)$, $(\sqrt{3} \times \sqrt{3})30^\circ$, and $(3/2 \times 3/2)$ adsorption structures consists of nine copper atoms in each substrate layer. For the $p(2 \times 2)$ structure we use a supercell with four Cu atoms per layer. The Na adatoms are arranged in a corresponding adsorption structure on both terminations of the slab.

The considered adsorption configurations are shown in Fig. 1. The structures corresponding to a submonolayer coverage of Na were suggested as a possible model of the transition from the $p(3 \times 3)$ phase with one Na atom per unit cell, which is locally formed by sodium adsorbates at low coverage (0.25 ML), to the $(3/2 \times 3/2)$ structure with four Na atoms per unit cell, which is formed at monolayer saturation.²³ Such a model was motivated by an analysis of the electronic structure of the Na films. Since preferable adsorption sites for sodium on Cu(111) are still under discussion, we first considered top, bridge, and hollow positions to calculate the corresponding binding energies for Na adatoms. The obtained results are close to the first-principles data reported by Carlsson and Hellsing⁹ for the structures $p(2 \times 2)$ and $(3/2 \times 3/2)$. The energy differences between distinct adatom positions are very small, so it is difficult to determine the preferable adsorption site, though, in the low-coverage range, the hollow sites seem to be more favorable. As for the fcc or hcp position of Na adatoms, the obtained binding energies are almost the same for all the adsorption structures considered. The surface relaxations with Na in fcc and hcp hollow sites coincide within a few hundredths of a percent. We have also performed phonon calculations with the sodium atoms on the top positions and in both fcc and hcp hollow adsorption sites. It was found that the choice of a hollow site type had practically no effect on phonon spectra while for structures with Na on the top positions imaginary phonon frequencies appeared as an indication of the crystal structure instability. So the results presented below are obtained with Na placed in the fcc hollow sites. In the case of the $(3/2 \times 3/2)$ structure there is no possibility to construct a hexagonal adlayer using only one type of adatom site: the chosen configuration [Fig. 1(d)] has atom 1 in the fcc hollow site and atoms 2, 3, and 4 in the surface unit cell at displaced hcp hollow positions.

III. RESULTS

A. Clean Cu(111) surface

For the clean Cu(111) surface the first interlayer spacing as well as the second one were found to be contracted compared to the bulk interlayer distance, $\Delta_{12} = -1.05\%$ and $\Delta_{23} = -0.07\%$. This is in agreement with available experimental and computational data. The relative contractions of the interlayer distance measured using medium-energy ion scattering were found to be $\Delta_{12} = -1.0\% \pm 0.4\%$, and $\Delta_{23} = -0.2\% \pm 0.4\%$.⁴² The values obtained in the semiempirical³⁸ and first-principles calculations⁴³ are $\Delta_{12} = -1.14\%$ and Δ_{12}

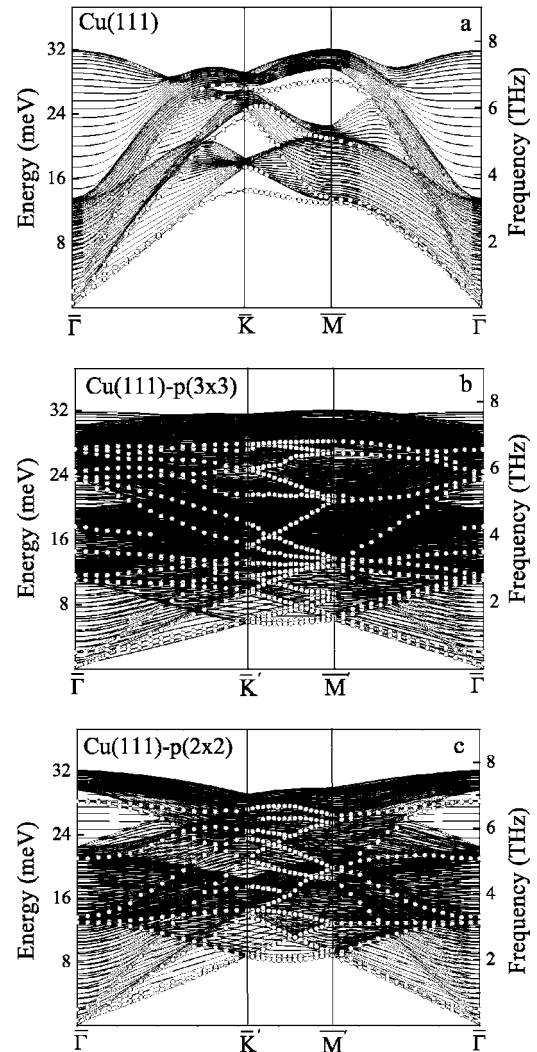


FIG. 2. Phonon dispersion curves for the Cu(111) surface with (a) (1×1) , (b) (3×3) , and (c) (2×2) unit cells. The open circles show the surface states.

$= -0.9\%$, respectively. The calculated phonon dispersion curves along the high-symmetry directions of the irreducible part of the two-dimensional Brillouin zone (BZ) are shown in Fig. 2(a) (surface modes are denoted by open circles). The obtained vibrational energies for the Rayleigh mode (RW) at the high-symmetry points \bar{K} (14.5 meV) and \bar{M} (13.03 meV) agree well with both experimental data^{44,45} (14.06 and 13.24 meV, respectively) and theoretical results reported in Ref. 43 (15.3 and 13.5 meV) and Ref. 46 (14.06 and 13.65 meV).

To compare directly the phonon spectra of the clean and adsorbate-covered surfaces we calculated first the phonons for the clean surface with (2×2) and (3×3) unit cells. The corresponding BZ's are shown in Fig. 3 in comparison with that of the conventional (1×1) unit cell. In the (3×3) case, the BZ is nine times less than that of the (1×1) unit cell. This implies that different points of the original (1×1) BZ are folded into the same symmetry points of the smaller $p(3 \times 3)$ BZ as follows:

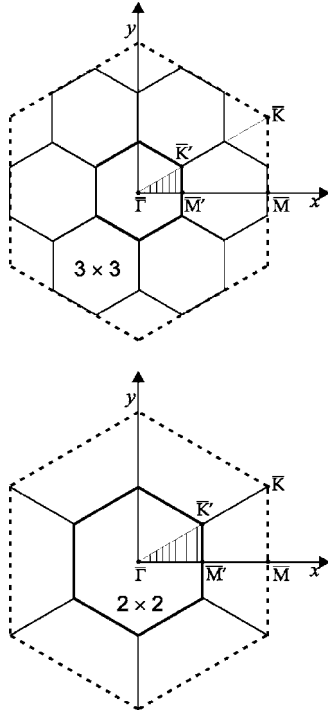


FIG. 3. Surface Brillouin zone for the (1×1) , (3×3) , and (2×2) surface structures. The irreducible part of the BZ's for the (3×3) and (2×2) structures is hatched. Dashed hexagons correspond to the BZ of the (1×1) unit cell.

$$(3 \times 3) \begin{cases} \bar{\Gamma}, \bar{K}, \frac{2}{3}\bar{\Gamma M} \rightarrow \bar{\Gamma}', \\ \bar{M}, \frac{1}{3}\bar{\Gamma M}, \frac{1}{2}\bar{\Gamma K} \rightarrow \bar{M}', \\ \frac{1}{3}\bar{\Gamma K}, \frac{2}{3}\bar{\Gamma K}, \frac{1}{3}\bar{M K} \rightarrow \bar{K}', \end{cases}$$

where $\frac{2}{3}\bar{\Gamma M}$ means two-thirds of the segment $\bar{\Gamma M}$, etc. As a consequence, the number of phonon branches for the $p(3 \times 3)$ structure, displayed in Fig. 2(b), is nine times that for the original (1×1) surface. For example, at the $\bar{\Gamma}$ point two of the folded surface modes with a vertical (z) polarization originate from the RW modes at the points $\frac{2}{3}\bar{\Gamma M}$ (11 meV) and (\bar{K}) (14.5 meV) of the original (1×1) BZ. Similarly at the \bar{M}' point one can find the surface modes from the points \bar{M} , $\frac{1}{3}\bar{\Gamma M}$, and $\frac{1}{2}\bar{\Gamma K}$ of the original unfolded BZ. For the $p(2 \times 2)$ BZ the folding scheme is

$$(2 \times 2) \begin{cases} \bar{\Gamma}, \bar{M} \rightarrow \bar{\Gamma}', \\ \frac{1}{2}\bar{\Gamma M}, \frac{3}{4}\bar{\Gamma K} \rightarrow \bar{M}', \\ \bar{K}, \frac{1}{2}\bar{\Gamma K} \rightarrow \bar{K}', \end{cases}$$

and the corresponding phonon branches, displayed in Fig. 2(c), are four times as many as in the original (1×1)

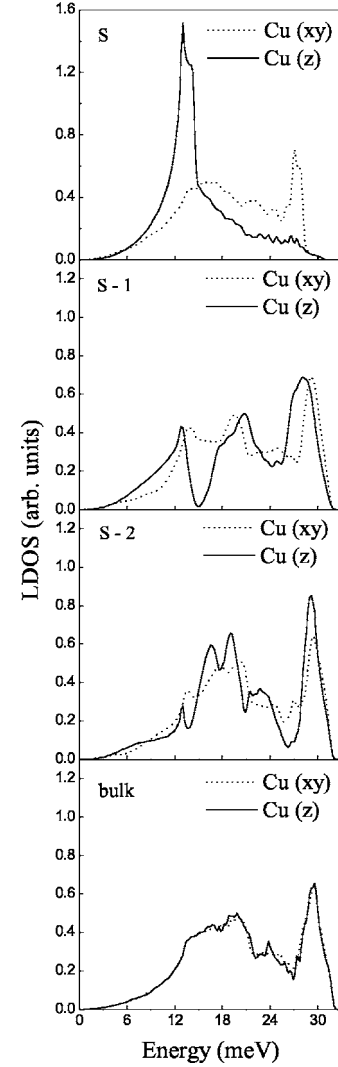


FIG. 4. Local density of states for the clean Cu(111) surface.

structure. In Fig. 4 we plot the local density of states (LDOS) for the outermost three layers of the surface as well as for the central layer. The calculated LDOS's show features quite typical for the (111) fcc surface.⁴⁷ Further, we will discuss the alterations of the surface modes and LDOS's that are inherent to the clean Cu(111) surface and the appearance of new surface modes due to the Na adsorption.

B. Cu(111)- $p(3 \times 3)$ -Na

First we consider a $p(3 \times 3)$ structure with one atom per unit cell [Fig. 1(a)] that is locally formed at a low coverage of sodium, $\theta \approx 0.11$ (0.25 of the saturated monolayer).²³ The Na atoms were arranged above the hollow sites of the relaxed Cu(111) substrate in a $p(3 \times 3)$ structure. Then the atoms were allowed to move according to the calculated forces until the equilibrium positions were achieved. The calculated bond length between the Na adatom and its nearest-neighbor Cu atom, $d_{\text{Na-Cu}}$, is 2.82 Å. Unfortunately there are neither experimental data nor theoretical results for the bond length in this structure. On the other hand, $d_{\text{Na-Cu}}$ obtained from a density-functional theory (DFT) calculation for sodium in

TABLE I. The coordinates of sodium adatoms and the first-layer substrate atoms after relaxation. The coordinates are given with respect to the ideal center of mass of the three Cu atoms creating the hollow site before relaxation. The numbering of the atoms can be seen in Fig. 1. Δx and Δy are atomic displacements from the ideal positions due to relaxation. In parentheses *ab initio* calculation results are given.

Atom	x (Å)	Δx	x (Ref. 9)	y (Å)	Δy	y (Ref. 9)	z (Å)	z (Ref. 9)
Hollow site, Cu(111)- $p(3 \times 3)$ -Na								
Cu ₁	-1.290	-0.012		-0.745	-0.007		-0.053	
Cu ₂	1.290	0.012		-0.745	-0.007		-0.053	
Cu ₄	0.000	0.000		1.489	0.014		-0.053	
Na	0.000	0.000		0.000	0.000		2.342	
Hollow site, Cu(111)- $p(2 \times 2)$ -Na								
Cu ₁	-1.287	-0.009	(-1.31)	-0.743	-0.005	(-0.75)	-0.028	(0.00)
Cu ₂	1.287	0.009	(1.30)	-0.743	-0.005	(-0.75)	-0.028	(0.00)
Cu ₃	0.000	0.000	(0.00)	1.487	0.011	(1.51)	-0.028	(0.00)
Cu ₄	2.547	0.000	(2.59)	1.476	0.000	(1.49)	0.056	(0.08)
Na	0.000	0.000	(0.00)	0.000	0.000	(0.00)	2.387	(2.40)
Hollow site, Cu(111)-($\sqrt{3} \times \sqrt{3}$)-Na								
Cu ₁	-1.296	-0.018		-0.748	-0.010		-0.007	
Cu ₂	1.296	0.018		-0.748	-0.010		-0.007	
Cu ₄	0.000	0.000		1.496	0.020		-0.007	
Na	0.000	0.000		0.000	0.000		2.416	
Hollow site, Cu(111)-($3/2 \times 3/2$)-Na								
Cu ₁	-1.294	-0.016	(-1.31)	-0.747	-0.009	(-0.76)	0.032	(0.04)
Cu ₂	1.294	0.016	(1.31)	-0.747	-0.009	(-0.76)	0.032	(0.04)
Cu ₄	0.000	0.000	(0.00)	1.495	0.019	(1.51)	0.032	(0.04)
Na ₁	0.000	0.000	(0.00)	0.000	0.000	(0.00)	2.477	(2.51)
Distorted hollow site, Cu(111)-($3/2 \times 3/2$)-Na								
Cu ₃	0.000	0.000	(0.00)	-0.760	-0.022	(-0.77)	-0.097	(-0.10)
Cu ₅	-1.285	-0.006	(1.29)	1.472	-0.004	(1.49)	0.059	(0.05)
Cu ₆	1.285	0.006	(1.30)	1.472	0.004	(1.49)	0.059	(0.05)
Na ₂	0.000	0.000	(0.00)	0.040	0.040	(0.08)	2.459	(2.47)

hollow sites at coverages of 0.56 and 1 ML (2.84 and 2.87 Å, respectively) was found to increase with increasing coverage.⁹ So the calculated bond length for a 0.25 ML Na film is quite plausible. As a result of Na adsorption a small rumpling in the first two layers of the substrate arises. The Cu surface atoms located beneath the Na adatoms are repelled into the substrate by 0.05 Å, while other surface copper atoms move outward by 0.01 Å. Taking into account the rumpling in the second substrate layer, the resulting relative changes of the first and the second substrate interlayer distances with respect to the bulk spacing are $\Delta_{12} = -1.93\%$ and $\Delta_{23} = -0.75\%$ in the vicinity of the adatoms and $\Delta_{12} = -0.84\%$ and $\Delta_{23} = 0.72\%$ otherwise. The optimized coordinates of the adsorbate and surface atoms are given in Table I.

The calculated phonon dispersion curves for Cu(111)- $p(3 \times 3)$ -Na are shown in Fig. 5. All the surface states found on the clean Cu(111) surface remain, including the RW modes. The presence of adsorbates leads to a small alteration of their frequencies while the polarizations are not affected. Some of the modes have now a mixed character with displacements of both adatoms and substrate atoms. Thus, the vibrational energies of the two lowest substrate surface pho-

non modes associated mainly with vertical displacements of atoms (these modes lie at the edge of the bulk spectrum) become somewhat smaller than they are in the case of the clean Cu(111), while the vibrational energies of the two highest substrate surface modes which correspond to in-plane motion of atoms are slightly higher than those on the clean Cu(111). The Na adsorption also gives rise to two new surface modes below the bottom of the bulk spectrum. They

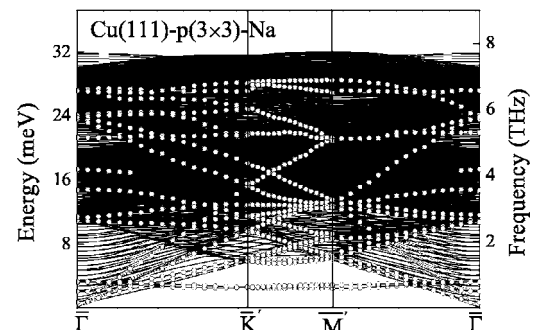
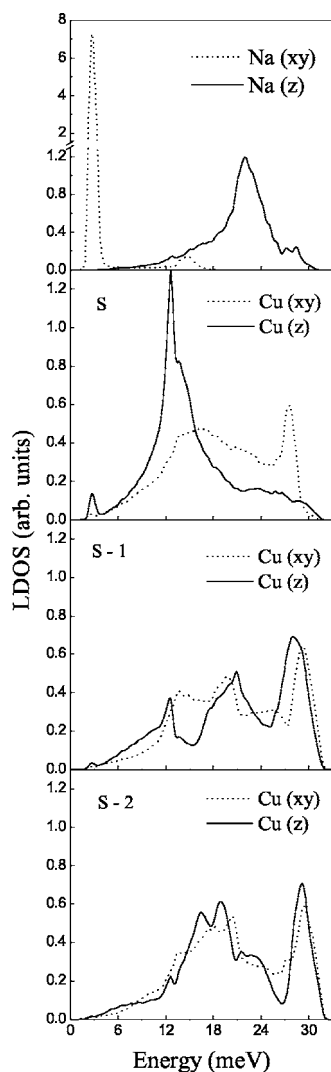
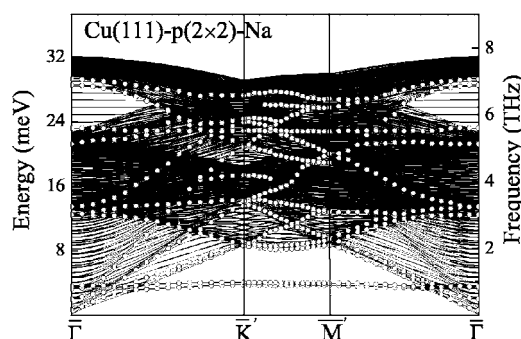


FIG. 5. Phonon dispersion curves for Cu(111)- $p(3 \times 3)$ -Na. The open circles show surface states.

FIG. 6. Local density of states for Cu(111)- $p(3 \times 3)$ -Na.

extend over the entire BZ and are almost dispersionless. These frustrated translation (T) modes associated with in-plane displacements are mainly localized on the adatoms though on moving to the zone center they couple to the vertical and in-plane motion of the substrate atoms the corresponding small peaks at 3 meV are clearly seen in the local density of states for the surface (S) and subsurface ($S-1$) substrate layers (Fig. 6). The obtained “splitting” of the adlayer T modes is related to their hybridization with the substrate acoustic modes: one T mode couples to the in-plane substrate modes, whereas the other T mode couples to the shear-vertical ones. When this coupling becomes negligible, as happens when the T modes fall outside the bulk continuum, they become almost degenerate. Another mode was obtained at the $\bar{\Gamma}$ point at an energy of 21.92 meV. This adsorbate-induced resonance characterized by displacements of adatoms along the surface normal involves both in-plane and vertical transverse motion of the substrate Cu atoms. It spreads along all the high-symmetry directions of the BZ, merging with the surface substrate phonons on moving to the zone boundaries. A similar mode was obtained experimentally using EELS.³⁶ Its vibrational energy of ~ 21.0 meV was

FIG. 7. Phonon dispersion curves for Cu(111)- $p(2 \times 2)$ -Na. The open circles show surface states.

measured at coverages of up to 0.35 ML and found to be almost constant. However, a strongly coverage-dependent intensity was observed with a maximum at ~ 0.15 – 0.20 ML. In Fig. 6 the calculated local density of states is presented for the first three layers of the substrate and for adatoms. As one can see, the substrate LDOS’s do not change significantly at this coverage as compared with the clean surface except for a very small additional peak which appears at low energies for z -polarized vibrations of the top-layer Cu atoms (S) as well as for the subsurface Cu atoms ($S-1$). These new substrate modes are mixing with the in-plane vibrations of Na adatoms mentioned above. The vertical vibrations of adsorbates form a strong peak in the LDOS around the energy of 22 meV.

C. Cu(111)- $p(2 \times 2)$ -Na

For a sodium coverage of $\theta \approx 0.25$ (0.56 of the saturated monolayer), it was suggested that the adsorbates form an ordered $p(2 \times 2)$ structure [Fig. 1(b)].^{19,20,23} After relaxation, the bond length between the Na adatom and its nearest-neighbor substrate atom, $d_{\text{Na-Cu}}$, is found to be of 2.84 Å. This result coincides with the value obtained in the DFT calculation for this adsorption system.⁹ As in the previous case, a small tendency for the substrate rumpling is found, i.e., the substrate atoms located below the sodium adatoms are repelled into the substrate by 0.03 Å, while the others move outward by 0.06 Å (see Table I). For Cu(111)- $p(2 \times 2)$ -Na the relative changes of the first and second interlayer spacings for the Cu atoms arranged around the Na adatom are found to be $\Delta_{12} = -1.1\%$, and $\Delta_{23} = -0.35\%$ with respect to the bulk interlayer distance. The corresponding values for the substrate atoms situated in the center of the Na triangle [atom 4 in Fig. 1(b)] are 2.13% and -0.12% , respectively.

The phonon dispersion curves for Cu(111)- $p(2 \times 2)$ -Na are shown in Fig. 7. As in the previous case, the most prominent feature is the lowest two T modes below the bulk phonons which are strongly localized on Na adatoms. Both of them correspond to in-plane vibrations of adsorbates. However, as one can find, they shift toward the higher energies and at the \bar{K}' and \bar{M}' symmetry points their vibrational energies are now 3.8–3.9 meV while in the case of the Cu(111)- $p(3 \times 3)$ -Na structure these modes were found at energies of about 2.2–2.5 meV. Another surface mode is a

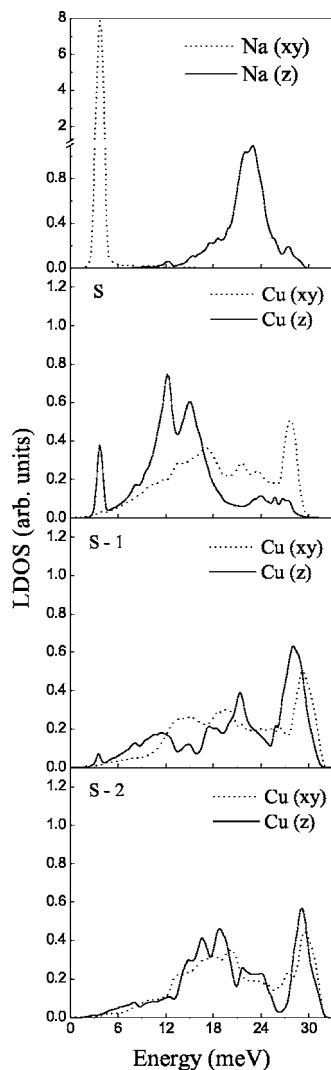


FIG. 8. Local density of states for Cu(111)- $p(2 \times 2)$ -Na.

vertically polarized resonance extending along all the symmetry directions of the BZ. The energy of this vibrational mode at the $\bar{\Gamma}$ point is ~ 22 meV. In the case of the Cu(111)- $p(3 \times 3)$ -Na structure this surface resonance was obtained at nearly the same energy. So its vibrational energy does not vary with increasing coverage as was found experimentally by Lindgren and Walldén.³⁶ As in the previous case, this mode involves in-plane as well as vertical vibrations of the Cu substrate atoms and couples to the surface substrate phonons on moving to the zone boundaries. In Fig. 8 we present the calculated local density of states for the Na adlayer and three substrate layers. For Na atoms the results are very similar to those obtained for the smaller coverage. The main features are a low-energy peak determined by in-plane motion of adsorbates and a broad peak distributed over a relatively large energy interval around 22 meV and corresponding to the vertical vibrations of adatoms. The latter is similar to that for the Cu(111)- $p(3 \times 3)$ -Na structure but it is now broader and less intensive. As for the LDOS's for the first two substrate layers, they change markedly. An additional low-energy peak at approximately 4 meV for vertically polarized vibrations of the top layer Cu atoms (S) be-

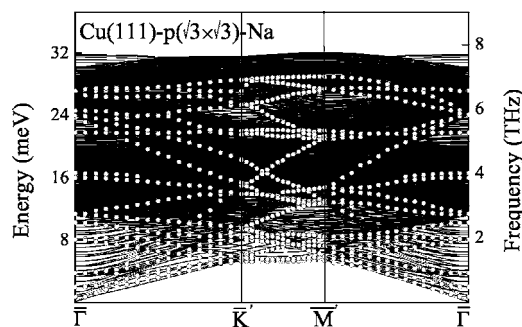


FIG. 9. Phonon dispersion curves for Cu(111)- $(\sqrt{3} \times \sqrt{3})30^\circ$ -Na. The open circles show surface states.

comes more pronounced. This peak is determined by the surface substrate modes which couple to the in-plane adsorbate motion and assume a mixed character as was mentioned in the previous case. The main peak associated with z -polarized vibrations of the first-layer Cu atoms splits up into two due to the hybridization with the adsorbate modes. The LDOS for the second substrate layer ($S-1$) assumes more bulklike features.

D. Cu(111)- $(\sqrt{3} \times \sqrt{3})30^\circ$ -Na

Now we consider an intermediate (3×3) phase with three Na atoms per unit cell, $(\sqrt{3} \times \sqrt{3})30^\circ$ -Na, suggested in Ref. 23 for coverage $\theta \approx 0.33$ (0.75 of the saturated monolayer). The calculated equilibrium bond length between the Na adatom and its nearest-neighbor substrate atom, $d_{\text{Na-Cu}}$, is found to be 2.85 Å. Unlike the previous cases no rumpling in the first substrate layer was obtained because all Cu atoms have the same atomic surrounding with regard to the adsorbates while in the second substrate layer a small rumpling remains. The relative changes of the first and the second interlayer spacings are $\Delta_{12} = -1.32\%$ and $\Delta_{23} = 0.59\%$, respectively.

The calculated phonon spectrum for Cu(111)- $(\sqrt{3} \times \sqrt{3})30^\circ$ -Na is shown in Fig. 9. In this case there are no modes below the bulk continuum. Unlike the previous structures, the T modes associated with the in-plane vibrations of sodium adatoms move up to higher energies. At the zone boundary they lie at the edge of the bulk spectrum and remain almost dispersionless. Their vibrational energies are of ~ 5.5 – 5.6 meV. On moving to the zone center these modes enter the bulk phonon region and split up. At the $\bar{\Gamma}$ point their vibrational energies are of 3.7 and 8.0 meV. This splitting is clearly seen in the local density of states shown in Fig. 10. The peak associated with the in-plane vibrations of the adsorbates becomes double. At energies of about 21.9–22.1 meV there is a strong surface resonance which spreads along all the symmetry directions of BZ. It is characterized by vertical displacements of Na adatoms mixed with the substrate atom vibrations. Similar modes were obtained for all other adsorption structures considered. Their vibrational energies practically do not change with coverage and agree well with the experimental value of 21 meV.³⁶ The narrow low-energy peak associated with the in-plane motion of adsorbates, which is a distinctive characteristic of the low-

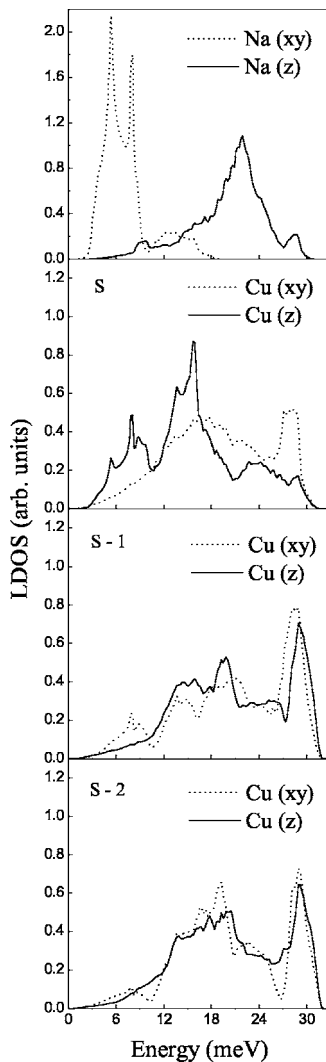


FIG. 10. Local density of states for Cu(111)- $(\sqrt{3} \times \sqrt{3})30^\circ$ -Na.

coverage structures, now splits and becomes broader and smaller due to the increasing hybridization with substrate modes. In addition, a second peak grows in the energy range of 12–16 meV. It is determined by in-plane adsorbate vibrations which couple to the RW modes of the Cu substrate. As for the top substrate layer, the corresponding LDOS changes for the vibrations along the surface normal. On the whole, the peaks are shifted towards higher energies and, besides, the lower one associated with the substrate atom vibrations which couple to the in-plane motion of the adatoms broaden out considerably. As follows from Fig. 10, LDOSs for the second and third substrate layers are already bulklike.

E. Cu(111)-(3/2×3/2)-Na

The structure which Na adatoms form at the monolayer saturation (it occurs at the coverage $\theta \approx 0.44$) has a (3×3) hexagonal symmetry with four Na atoms per unit cell.^{21,23} The nearest-neighbor distance between Na atoms was found to be 3.78 Å that is very close to the metallic diameter of sodium.³ In the calculations we used a supercell consisting of

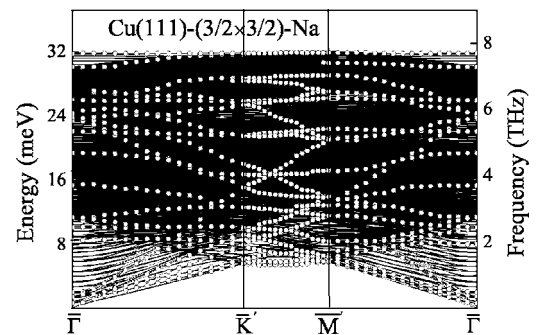


FIG. 11. Phonon dispersion curves for Cu(111)-(3/2×3/2)-Na. The open circles show surface states.

nine Cu atoms in each substrate layer and four Na atoms placed in the hollow-site-center adsorption structure: one hollow site [atom 1 in Fig. 1(d)] surrounded by six distorted hollow sites.⁹ The atomic positions of the adsorbate and substrate atoms were then relaxed to optimize the interlayer distances and take into account surface reconstruction effects. The obtained coordinates are shown in Table I. The calculated nearest-neighbor Na-Cu distance $d_{\text{Na-Cu}}$ is 2.87 Å for Na atoms in hollow sites and 2.68 Å for Na atoms in distorted hollow sites. This result is in a good agreement with the first-principles calculation values, $d_{\text{Na-Cu}} = 2.89$ Å (hollow site) and $d_{\text{Na-Cu}} = 2.71$ Å (distorted hollow site).⁹ Another result of the relaxation is a small substrate rumpling. The Cu atoms lying just below the sodium one in the hollow site [atoms 1, 2, and 4 in Fig. 1(d)] are shifted up by 0.03 Å. Atoms 5, 6, and 8 are moved up too but the displacement value is 0.06 Å while the substrate atoms below the sodium adatoms in the distorted hollow sites (atoms 3, 7, and 9) are shifted down by 0.10 Å. Taking into account the rumpling in the second substrate layer the final relative change of the first interlayer Cu spacing, Δ_{12} , is 0.53% in the vicinity of the sodium atom in a hollow site and $\Delta_{12} = -0.09\%$ for substrate atoms 5, 6, and 8. Close to the Na adatoms in the distorted hollow sites (Cu atoms 3, 7, and 9) the first substrate interlayer distance contracts by 5.04% compared to the bulk value.

The calculated phonon spectrum is shown in Fig. 11. As for case of the Cu(111)- $(\sqrt{3} \times \sqrt{3})30^\circ$ -Na structure, no Na modes appear below the bottom of the bulk phonons. However, a new surface mode and a surface resonance appear at the top of the bulk spectrum. The surface mode is characterized by both in-plane and vertical transverse vibrations of the surface and subsurface Cu atoms as well as by the shear-vertical motion of adatoms in the distorted hollow sites. The resonance, the highest-phonon mode in the $\Gamma K'$ and $\Gamma M'$ directions, is related to the transverse motion of the substrate atoms only. An analysis of the interatomic force constants shows that the interaction between an adsorbate in the hollow position and the nearest-neighbor Cu atoms becomes weaker with the increasing coverage. However, in the case of the $(3/2 \times 3/2)$ structure three of four Na adatoms in the unit cell occupy distorted hollow sites and for them the interaction with the substrate is found to be strong. It is even stronger than the interlayer interaction between Cu atoms in the case of the clean Cu(111) surface. The interaction between

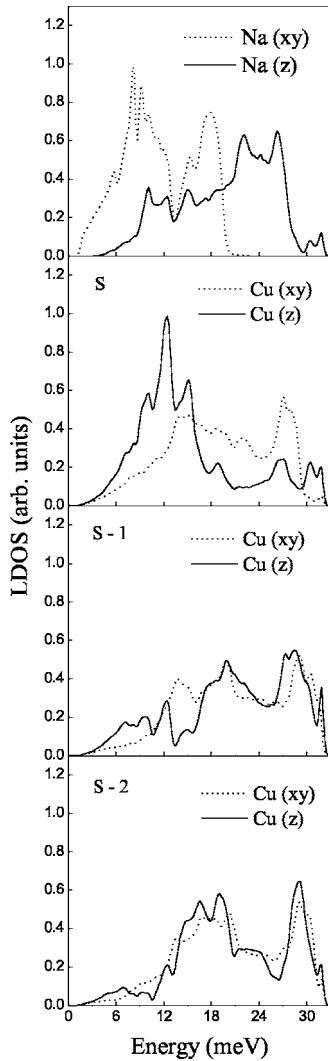


FIG. 12. Local density of states for Cu(111)-(3/2 × 3/2)-Na.

the surface and subsurface Cu atoms located below the sodium adatoms in the distorted hollow sites notably strengthens too unlike the previous cases. In particular, this results in the substantial contraction of the first interlayer substrate spacing and the appearance of the high-energy mixed transverse modes at energies between 30 and 33 meV. As clearly seen in Fig. 12, these modes penetrate up to the third Cu layer. As in the previous cases a mixed surface state corresponding to the shear-vertical displacements of the adatoms in the hollow sites was obtained. This almost dispersionless mode extends along the entire BZ. Its vibrational energy does not change compared to that for the structures with the smaller coverage and amounts to 22.1 meV at the $\bar{\Gamma}$ point. The other adatoms, located in the distorted hollow sites, form a very flat mode of vertical vibrations at energy of approximately 26.3 meV. These two modes produce the corresponding two peaks in LDOS for the adatom layer (Fig. 12). A few new peaks of z -polarized adatom vibrations are seen in the LDOS at energies 9–16 meV. These vibrations couple to vertical motion of the Cu substrate atoms. In general, the 1 ML Na/Cu(111) LDOS for z -polarized vibrations of adatoms is much broader than the corresponding LDOS for the

lower coverages. This clearly shows that the vibrational spectrum of 1 ML of Na on Cu(111) is very different from the single mode spectrum which can be used for the simple description of the z -polarized Na vibrations at lower coverages. Additionally to the large broadening, the LDOS for the Na vertical vibrations appears to be significantly smaller in magnitude compared to that for the lower coverages. Two T modes associated with in-plane displacements of adsorbates are shifted toward the higher energies above the bulk phonon edge. The first of them is mainly determined by the in-plane displacements of the hollow site adsorbates (84%), the second one is characterized by the in-plane motion of the Na atoms in the distorted hollow positions (66%). Both modes couple to the motion of the top layer Cu atoms along the surface normal. At the \bar{M}' point the vibrational energies of these modes are 5.87 and 6.41 meV, respectively. Approaching the \bar{K}' point they degenerate and have a vibrational energy of about 8.0 meV. Then, as in the case of the $(\sqrt{3} \times \sqrt{3})$ structure, they split on moving to the zone center and at the $\bar{\Gamma}$ point these modes are located about energies of 1.5 and 8.5 meV, respectively. In contrast to in-plane vibrations of adsorbates at low coverages of Na, for 1 ML Na an additional strong peak in the LDOS appears at energy of approximately 18 meV. This peak is determined by the adlayer vibrations which couple to the RW modes of the Cu substrate.

IV. CONCLUSION

We have presented the results of a comparative study of the vibrational and structural properties of the Na/Cu(111) systems at coverages up to the monolayer saturation. The following ordered structures have been considered: $p(3 \times 3)$, $p(2 \times 2)$, $(\sqrt{3} \times \sqrt{3})30^\circ$, and $(3/2 \times 3/2)$ corresponding to coverages of 0.25, 0.56, 0.75, and 1 ML of Na, respectively. The calculation of equilibrium geometry showed that the bond length between an adsorbate and the nearest-neighbor substrate atom slightly increases with increasing coverage. The obtained bond lengths for the $p(2 \times 2)$ and $(3/2 \times 3/2)$ structures are in good agreement with the *ab initio* results.⁹ Adsorption of sodium also results in a small rumpling in the two substrate layers. The magnitudes of these local alterations depend on the relative positions of Cu atoms with respect to the adsorbates.

All the surface modes inherent in the clean Cu(111) surface were found to remain at any coverage. They only assume a mixed character coupling to the adsorbate modes. The presence of adsorbates also leads to a small alteration of their frequencies. Marked changes occur for the z -polarized vibrations of the top Cu layer. With increasing coverage the corresponding peak in the LDOS splits up and broadens considerably due to hybridization with adsorbate atom motions. The mode associated with adatom-substrate stretch vibrations was obtained in our calculation at about 22 meV for all the structures considered. The calculated vibrational energy agrees well with the value of 21 meV measured by EELS and was found to be almost constant for any submonolayer coverage.³⁶ However, the intensity of this mode decreases by a factor of 2 with increasing coverage from 0.25 ML to the

saturated monolayer, which is also in agreement with experiment. At the saturated monolayer many maxima appear in the LDOS for z -polarized vibrations of adatoms, making the LDOS much broader than for lower coverages. One of these maxima corresponding to the vibrations of adsorbates in the hollow positions remains at about 22 meV. The sodium atoms located in the distorted hollow sites interact more strongly with the substrate due to the shorter Na-Cu distances and as a result have higher vibrational energies. Two adlayer T modes with in-plane polarization are located below the bottom of the bulk phonons for the $p(3 \times 3)$ and $p(2 \times 2)$ structures. As for their energies they are shifted up with increasing coverage. The “splitting” of these T modes is caused by hybridization with the substrate acoustic modes. When they fall outside the bulk continuum, they become almost degenerate. These modes appear in the corresponding LDOS's as narrow prominent peaks. The same modes for the $(\sqrt{3} \times \sqrt{3})$ and $(3/2 \times 3/2)$ structures are shifted toward

higher energies above the bulk phonon edge. So, unlike the energy constancy of the surface resonance at the $\bar{\Gamma}$ point (the stretch S mode), the vibrational energy of the frustrated translation T modes is found to be strongly coverage dependent. It increases by a factor of 3 with increasing coverage from $\theta \approx 0.11$ to $\theta \approx 0.44$. This dependence is due to the fact that the distance between adatoms becomes shorter with increasing coverage and as a result the interaction in the adlayer film becomes stronger too.

ACKNOWLEDGMENTS

We acknowledge B. Hellsing for critical reading of the manuscript and fruitful discussions. This work was supported by the Ministry of Science of Russia (Grant No. 02.434.11.2027) and NATO science program (Grant No. PST.CLG.980395).

*Electronic address: waptctce@sq.ehu.es

- ¹*Physics and Chemistry of Alkali Metal Adsorption*, edited by H. P. Bonzel, A. M. Bradshaw, and G. Ertl (Elsevier, Amsterdam, 1989).
- ²H. Tochihara and S. Mizuno, *Prog. Surf. Sci.* **58**, 1 (1998).
- ³R. D. Diehl and R. McGrath, *Surf. Sci. Rep.* **23**, 43 (1996).
- ⁴E. V. Chulkov and V. M. Silkin, *Surf. Sci.* **215**, 385 (1989).
- ⁵C. Stampfl, K. Kambe, R. Fasel, P. Aebi, and M. Scheffler, *Phys. Rev. B* **57**, 15251 (1998).
- ⁶S.-Å. Lindgren and L. Walldén, *Phys. Rev. B* **38**, 3060 (1988).
- ⁷N. Fischer, S. Schuppler, R. Fischer, Th. Fauster, and W. Steinmann, *Phys. Rev. B* **47**, 4705 (1993).
- ⁸A. Carlsson, B. Hellsing, S.-Å. Lindgren, and L. Walldén, *Phys. Rev. B* **56**, 1593 (1997).
- ⁹J. M. Carlsson and B. Hellsing, *Phys. Rev. B* **61**, 13973 (2000).
- ¹⁰G. Butti, S. Caravati, G. P. Brivio, M. I. Trioni, and H. Ishida, *Phys. Rev. B* **72**, 125402 (2005).
- ¹¹P. M. Echenique, R. Berndt, E. V. Chulkov, Th. Fauster, A. Goldman, and U. Höfer, *Surf. Sci. Rep.* **52**, 219 (2004).
- ¹²E. V. Chulkov, J. Kliewer, R. Berndt, V. M. Silkin, B. Hellsing, S. Crampin, and P. M. Echenique, *Phys. Rev. B* **68**, 195422 (2003).
- ¹³B. Hellsing, J. Carlsson, L. Walldén, and S.-Å. Lindgren, *Phys. Rev. B* **61**, 2343 (2000).
- ¹⁴For a review, see B. Hellsing, A. Eiguren, and E. V. Chulkov, *J. Phys.: Condens. Matter* **14**, 5959 (2002).
- ¹⁵C. Corriol, V. M. Silkin, D. Sánchez-Portal, A. Arnau, E. V. Chulkov, P. M. Echenique, T. von Hofe, J. Kliewer, J. Kröger, and R. Berndt, *Phys. Rev. Lett.* **95**, 176802 (2005).
- ¹⁶J. Neugebauer, M. Scheffler, *Phys. Rev. B* **46**, 16067 (1992).
- ¹⁷T. Nagao, Y. Iizuka, T. Shimazaki, and C. Oshima, *Phys. Rev. B* **55**, 10064 (1997).
- ¹⁸G. G. Rusina, S. V. Ereemeev, S. D. Borisova, I. Yu. Sklyadneva, and E. V. Chulkov, *Phys. Rev. B* **71**, 245401 (2005).
- ¹⁹S.-Å. Lindgren and L. Walldén, *Phys. Rev. B* **22**, 5967 (1980).
- ²⁰R. Dudde, L. S. O. Johansson, and B. Reihl, *Phys. Rev. B* **44**, 1198 (1991).
- ²¹D. Tang, D. McIlroy, X. Shi, C. Su and D. Heskett, *Surf. Sci. Lett.* **255**, L497 (1991).
- ²²N. Fischer, S. Schuppler, Th. Fauster, and W. Steinmann, *Surf. Sci.* **314**, 89 (1994).
- ²³J. Kliewer and R. Berndt, *Surf. Sci.* **477**, 250 (2001).
- ²⁴D. L. Adler, I. R. Collins, X. Liang, S. J. Murray, G. S. Leatherman, K.-D. Tsuei, E. E. Chaban, S. Chandavarkar, R. McGrath, R. D. Diehl, and P. H. Citrin, *Phys. Rev. B* **48**, 17445 (1993).
- ²⁵S.-Å. Lindgren, L. Walldén, J. Rundgren, P. Westrin, and J. Neve, *Phys. Rev. B* **28**, 6707 (1983).
- ²⁶X. Shi, C. Su, D. Heskett, L. Berman, C. C. Kao, and M. J. Bedzyk, *Phys. Rev. B* **49**, 14638 (1994).
- ²⁷S.-Å. Lindgren, C. Svensson, L. Walldén, A. Carlsson, and E. Wahlstrom, *Phys. Rev. B* **54**, 10912 (1996).
- ²⁸S. Mizuno, H. Tochihara, A. Barbieri, and M. A. Van Hove, *Phys. Rev. B* **51**, 7981 (1995).
- ²⁹L. Padilla-Campos, A. Toro-Labbe, and J. Maruani, *Surf. Sci.* **408**, 72 (1998).
- ³⁰G. Benedek, J. Ellis, A. Reichmuth, P. Ruggerone, H. Schief, and J. P. Toennies, *Phys. Rev. Lett.* **69**, 2951 (1992).
- ³¹G. Witte and J. P. Toennies, *Phys. Rev. B* **62**, R7771 (2000).
- ³²N. S. Luo, P. Ruggerone, and J. P. Toennies, *Phys. Rev. B* **54**, 5051 (1996).
- ³³C. Astaldi, P. Rudolf, and S. Modesti, *Solid State Commun.* **75**, 847 (1990).
- ³⁴P. Rudolf, C. Astaldi, G. Gautero, and S. Modesti, *Surf. Sci.* **251/252**, 127 (1991).
- ³⁵S.-Å. Lindgren, C. Svensson, and L. Walldén, *Phys. Rev. B* **42**, 1467 (1990).
- ³⁶S.-Å. Lindgren and L. Walldén, *J. Electron Spectrosc. Relat. Phenom.* **64/65**, 483 (1993).
- ³⁷A. P. Graham, J. P. Toennies, and G. Benedek, *Surf. Sci.* **556**, L143 (2004).
- ³⁸S. M. Foiles, M. I. Baskes, and M. S. Daw, *Phys. Rev. B* **33**, 7983 (1986).
- ³⁹I. Yu. Sklyadneva, E. V. Chulkov, and A. V. Bertsch, *Surf. Sci.* **352-354**, 25 (1996).
- ⁴⁰I. Yu. Sklyadneva, G. G. Rusina, and E. V. Chulkov, *Surf. Sci.*

- 416**, 17 (1998).
- ⁴¹R. A. Johnson, Phys. Rev. B **39**, 12554 (1989).
- ⁴²K. H. Chae, H. C. Lu, and T. Gustafsson, Phys. Rev. B **54**, 14082 (1996).
- ⁴³K. P. Bohnen and K. M. Ho, Surf. Sci. Rep. **19**, 99 (1993).
- ⁴⁴M. H. Mohamed, L. L. Kesmodel, Burl M. Hall, and D. L. Mills, Phys. Rev. B **37**, 2763 (1988).
- ⁴⁵U. Harten, J. P. Toennies, and Ch. Wöll, Faraday Discuss. Chem. Soc. **80**, 137 (1985).
- ⁴⁶Y. Chen, S. Y. Tong, K. P. Bohnen, T. Rodach, and K. M. Ho, Phys. Rev. Lett. **70**, 603 (1993).
- ⁴⁷R. E. Allen, G. P. Alldredge, and F. W. de Wette, Phys. Rev. B **4**, 1661 (1971).